

Mediator-lipidomics: databases and search algorithms for PUFA-derived mediators[§]

Yan Lu,¹ Song Hong,¹ Eric Tjonahen, and Charles N. Serhan²

Center for Experimental Therapeutics and Reperfusion Injury, Department of Anesthesiology, Perioperative and Pain Medicine, Brigham and Women's Hospital and Harvard Medical School, Boston, MA 02115

Abstract Lipid mediators (LMs) derived from PUFAs play important roles in health and disease. Databases and search algorithms are crucial, but currently unavailable, for accurate and prompt analysis of LMs via liquid chromatography-ultraviolet-tandem mass spectrometry (LC-UV-MS/MS). A novel algorithm and databases, cognoscitive-contrast-angle algorithm and databases (COCAD), were developed for the identification of LMs based on the integration of standard MS/MS spectra with chromatograms and UV spectra. Segment naming and empirical fragmentation rules were introduced to determine MS/MS ion identities, along with ion intensities used by COCAD in matching the unknown to those of authentic standards. The structures of potential LMs without synthetic and/or authentic products as standards were identified by developing theoretical databases and algorithms based on virtual LC-UV-MS/MS spectra and chromatograms. The performance of these databases and algorithms was tested by identifying LMs in murine tissues. These results indicate that COCAD has many advantages for profiling and identification of LMs compared with the conventional dot-product algorithm.—Lu, Y., S. Hong, E. Tjonahen, and C. N. Serhan. Mediator-lipidomics: databases and search algorithms for PUFA-derived mediators. *J. Lipid Res.* 2005. 46: 790–802.

Supplementary key words cognoscitive-contrast-angle algorithm and database • theoretical database and algorithm • inflammation • resolution • eicosanoids • resolvins • neuroprotectins • docosatrienes • polyunsaturated fatty acid

Lipid mediators (LMs) biosynthesized from precursor PUFAs such as eicosanoids, resolvins, neuroprotectins, and docosatrienes are local autacoids that play critical roles in human physiology and many prevalent diseases. These include cardiovascular disease, Alzheimer's disease, psoriasis, asthma, and arthritis as well as the physiologic events of inflammation and resolution (1–4). Lipidomics of LMs, namely the study of the identity, function, and profiling of potent bioactive LMs as well as their biosynthesis and metabolic inactivation, can provide a useful approach for qualifying LMs as diagnostic markers in metabolomics of dis-

ease and health and possibly in the development and assessment of new therapeutics (5, 6). As a subdivision of lipidomics, mediator-lipidomics is further subdivided into eicosanomics, which focuses on the classes of bioactive mediators derived from arachidonic acid, including, for example, prostaglandins (PGs), leukotrienes (LTs), lipoxins (LXs), epoxyeicosatrienoic acids, and isoeicosanoids, as well as LMs that are derived from other lipid structures, such as sphingolipids, diacylglycerides, lysophospholipids, and platelet-activating factors (for recent references, see 5, 6).

Although the physicochemical properties of individual LMs can give different chromatographic behaviors and mass spectra that are instrument- and chromatographic system-dependent, to facilitate profiling analyses between laboratories and assembling of system metabolomic maps, it is essential to first construct databases and search algorithms that permit accurate, prompt identification of LMs in complex biological matrices such as human blood, urine, and inflammatory exudates. To this end, one specific and sensitive tool for chemical identification in mediator-lipidomics is liquid chromatography-ultraviolet-tandem mass spectrometry (LC-UV-MS/MS) with atmospheric pressure ionization (7–10), especially electrospray ionization (ESI). Low-energy ionization of LMs with ESI generates primarily molecular (or pseudomolecular) ions for low/intermediate energy collision-induced dissociation (CID) MS/MS analysis and can avoid unwanted degradation products (7). MS/MS spectra are used extensively to identify and elucidate the structures of LMs derived from PUFAs (2–4,

Abbreviations: COCAD, cognoscitive-contrast-angle algorithm and databases; CRT, chromatographic retention time; ESI, electrospray ionization; HETE, hydroxy-eicosatetraenoic acid; LC-UV-MS/MS, liquid chromatography-ultraviolet-tandem mass spectrometry; LM, lipid mediator; LTB₄, 5S,12R-dihydroxy-6Z,8E,10E,14Z-eicosatetraenoic acid; LXA₄, 5S,6R,15S-trihydroxy-7E,9E,11Z,13E-trans-11-*cis*-eicosatetraenoic acid; LXB₄, 5S,14R,15S-trihydroxy-6E,8Z,10E,12E-eicosatetraenoic acid; PGE₂, 11α,15S-dihydroxy-9-oxo-prosta-5Z,13E-dien-1-oic acid; PGF_{2α}, 9α,11α,15S-trihydroxy-prosta-5Z,13E-dien-1-oic acid.

¹Y. Lu and S. Hong contributed equally to this work.

²To whom correspondence should be addressed.

e-mail: cnserrhan@zeus.bwh.harvard.edu

[§]The online version of this article (available at <http://www.jlr.org>) contains supplemental data.

Manuscript received 12 August 2004 and in revised form 12 January 2005.

Published, JLR Papers in Press, February 1, 2005.

DOI 10.1194/jlr.D400020-JLR200

7–9, 11). LC-UV-MS/MS can also provide more spectral information and criteria for those compounds with specific UV chromophores and assist in the elucidation of both known and novel LM structures. In this context, many LMs derived from PUFAs possess conjugated double bond systems that are critical components for their bioactions; each gives a characteristic UV spectrum (2–4, 7–9). Unesterified PUFAs frequently coexist in samples, and these compounds contain 1,4-*cis*-pentadiene subunits that do not give a specific UV chromophore signature. For example, leukotrienes contain a conjugated triene chromophore and lipoxins possess a conjugated tetraene chromophore.

Mediator-lipidomic databases containing MS/MS as well as UV spectra and chromatographic profiles with appropriate search algorithms are imperative for accurate and timely analysis of LMs (12). Mediator-lipidomic analysis is summarized in **Scheme 1**.

Although GC-MS can be used in many cases for structure identification, the required high column temperatures limit its use because many of the PUFA-derived LMs are thermolabile (7). Search algorithms for GC-MS electron impact ionization spectra have been well studied (13–15), as have those for both GC-MS chromatograms and mass spectra (16). The contrast-angle (or dot-product, = cosine of the contrast-angle) algorithm is widely used. The contrast-angle is the angle between two spectra represented as vectors composed of ordered peak intensities (13). Because databases and search algorithms for LMs on comprehensive LC-UV-MS/MS are not yet available, we initially used MassFrontier™ (ThermoFinnigan) GC-MS mass spectral commercial software to construct a LM database and search algorithm. The search algorithm for MassFrontier is dot-product and was developed by Stein and Scott (13, 14).

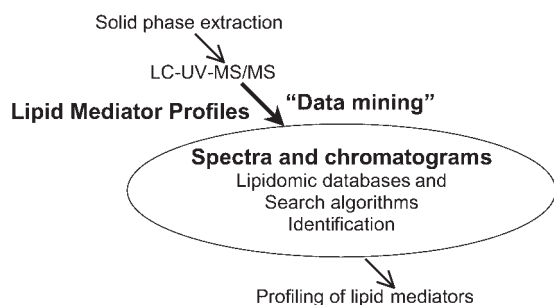
The dot-product algorithm in MassFrontier uses the intensities of all peaks in MS/MS as a vector for computation and is not concerned with the identities of ions, whether they are molecular ions, ions derived from molecular ions, or ions from interfering substances in the samples (13–16). Using the ions generated from interfering background can decrease the percentage correct for best match of the search. Even the ions generated from unknown LMs contribute differently to the identification. For LMs,

ions generated by cleavage of the carbon-carbon bond inside the carbon chain have greater diagnostic yield for determining the structures than the ions formed by the loss of water or CO₂, which are common features of most PUFA-derived LMs (3, 4, 7, 8, 11).

The relationships between ESI-MS/MS spectra and LM structures have been studied extensively (2–4, 7–9). The identification and elucidation of the unknown structures of novel LMs by LC-UV-MS/MS are based on the relationships between structural features (such as functional groups and double bonds) and characteristics of the spectra and chromatograms (MS/MS ions, UV spectra, and LC retention times). On C18 reversed-phase LC, chromatographic retention times (CRTs) generally increase in the following order: trihydroxy LMs, dihydroxy LMs, monohydroxy LMs, and then the nonoxidized PUFA precursors (such as arachidonic acid) are eluted, depending on the mobile phase used. For positional isomers of hydroxy-containing LMs, the CRTs decrease as the hydroxy groups locate closer to the methyl group at the ω -end of the long-chain PUFA. For instance, the CRT of 5*S*,14*R*,15*S*-trihydroxy-6*E*,8*Z*,10*E*,12*E*-eicosatetraenoic acid (LXB₄) is usually shorter than that of 5*S*,6*R*,15*S*-trihydroxy-7*E*,9*E*,11*Z*,13*E*-*trans*-11-*cis*-eicosatetraenoic acid (LXA₄). The CRT of native LXA₄ (containing a 15*S*-hydroxy at carbon 15) is shorter than that of the aspirin-triggered 15-*epi*-LXA₄ but greater than that of 11-*trans*-LXA₄, which is the natural all-*trans*-containing isomer of LXA₄ (17).

The band multiplicity and maximum absorbance wavelength (λ_{\max}) of UV spectra are additional class- or series-specific signatures of LMs, such as the presence of an asymmetric singlet band with $\lambda_{\max} \sim 235$ nm for the conjugated diene present within the lipoxygenase pathways. These include monohydroxy-eicosatetraenoic acids (mono-HETEs); a triplet with $\lambda_{\max} \sim 270$ nm for the leukotrienes, such as the conjugated triene within LTB₄ (5*S*,12*R*-dihydroxy-6*Z*,8*E*,10*E*,14*Z*-eicosatetraenoic acid); a triplet with $\lambda_{\max} \sim 300$ nm for conjugated tetraene, as present within LXA₄ and LXB₄; and, for example, an asymmetric singlet with $\lambda_{\max} \sim 242$ nm from the two conjugated dienes interrupted by a methylene group, as present in the double lipoxygenation product 5*S*,15*S*-di-HETE (17). For compounds without a class and/or series specific chromophore or with λ_{\max} in vacuum UV range (actually undetectable on our LC-UV-MS/MS instrument) such as 1,4-*cis*-pentadiene-containing PUFAs as well as some prostaglandins, namely PGE₂ (11 α ,15*S*-dihydroxy-9-oxo-prosta-5*Z*,13*E*-dien-1-oic acid) and PGF_{2 α} (9 α ,11 α ,15*S*-trihydroxy-prosta-5*Z*,13*E*-dien-1-oic acid), which do not possess conjugated double bond systems (17, 18), the UV chromophore component is not used for identification. When the conjugated tetraene of LXA₄ isomers is in the all-*trans* geometry, the λ_{\max} is shifted to 302 nm instead of 300 nm (17). The relationship between MS/MS spectra and LM structures is of interest and presented *vide infra*.

With current chemical analytical technologies, most LMs are identified manually by comparing the spectra and chromatographic behaviors acquired from sample tissues with those of authentic standards of known LMs; when au-



Scheme 1. Mediator-lipidomics via liquid chromatography-ultra-violet-tandem mass spectrometry (LC-UV-MS/MS) analysis of the physicochemical properties, including MS/MS and UV spectra and chromatographic profiles.

thentic standards are not available, as in the case of novel LMs and their metabolites, basic chemical structures can be obtained on the basis of the relationship between structures and features of their spectra and chromatographic behaviors compared with those of synthetic and biogenic products prepared to assist in the assignment. We routinely identify LMs by comparing the unknown spectra (MS/MS, GC-MS, and UV spectra) and CRTs with those of authentic and synthetic standards if available or with a theoretical database that consists of virtual UV and MS/MS spectra and CRTs for discovering potentially novel LMs (3, 4, 12) if standards are not available. We initially developed a theoretical database and algorithm according to the relationships between LM structures and their spectral and chromatographic characteristics (12). The proposed structures of novel potential LMs in the theoretical databases were based on PUFA precursors and established biosynthetic pathways.

In this report, we focus on constructing mediator-lipidomic databases and search algorithms useful for the identification of LM structures using LC-UV-MS/MS with the following objectives: 1) to assemble a database using currently available mass spectral software; 2) to construct a cognitive-contrast-angle algorithm and databases (COCAD) to improve the identification of LMs using MS/MS ion identities that currently cannot be determined with available software; and 3) to develop a theoretical database and algorithm for assessing potentially novel and/or unknown structures of LMs and their metabolites in biologic matrices. It is quite meaningful to develop mediator-lipidomic databases and algorithms using ion trap mass spectrometers that are relatively cheaper and popular. Moreover, the fragmentation rules and patterns for CID spectra from triple-quadrupole mass spectrometers, another popular MS instrument, are similar to those we encounter using the ion trap (7, 19, 20). The databases and algorithms described in this report should be a useful initiation that can be extended to other types of MS instruments.

SYSTEMS AND METHODOLOGY

LC-UV-MS/MS-based mediator-lipidomic analysis

Chromatograms and spectra of samples and standards were acquired in negative-ion mode using a Finnigan LC-UV-ESI-LCQ ion trap tandem mass spectrometer (ThermoFinnigan, San Jose, CA). The entire LC-UV-MS system control and data analysis were performed using Xcalibur® software 1.3 (ThermoFinnigan) (2–4, 11, 12).

We used a LUNA C18-2 (Phenomenex, Torrance, CA) column packed with 5 μ m spherical C-18 particles. The dimension was 100 mm (or 150 mm) long and 2 mm inner diameter. The column was kept in a column heater (30°C). The LC system used a P-4000 quaternary LC pump (ThermoFinnigan). When the column was 100 mm long, the mobile phase (methanol-water-acetic acid, 65:35:0.01) flowed at 0.2 ml/min in C channel from 0 to 8 min, linearly ramped to methanol in D channel from 8.01 to 30 min, eluted as methanol for 5 min, and finally eluted as C again. When the column was 150 mm, the mobile phase (methanol-water-acetic acid, 65:35:0.01) flow rate was 0.2 ml/min through the C

channel from 0 to 15 min, linearly ramped to methanol in D channel from 15.01 to 48 min, eluted as methanol for 8 min, and returned eluted as C again.

UV spectra were acquired using a tandem photodiode-array UV detector (UV-6000; ThermoFinnigan) that scanned from 200 to 360 nm. Samples were injected manually with a 7125E injector equipped with a 100 μ l loop (Rheodyne, Rohnert Park, CA). The injection volume was 20 μ l, and the amount of each LM and related compounds in each set of analyses ranged from 0.5 to 100.0 ng.

The ion source conditions for the LCQ were set as follows: electrospray voltage, 4.3 kV; heating capillary, 230°C and –39 V; tube lens offset, 60 V; sheath N₂ gas, 80 units (near 1.2 l/min); auxiliary N₂ gas, 3 units (0.045 l/min). The ion trap analyzer typically scanned from m/z 200 to 800 in MS mode to determine the m/z of ESI-ion source-generated ions. The parameters for MS/MS were as follows: damping and collision gas, He (at \sim 0.1 Pa); isolation width, m/z 1.5; collision time, 30 ms; normalized collision energy on base of the maximum available tickling voltage (5 V), \sim 38% for prostaglandins and dihydroxy- and trihydroxy-containing acyclic eicosanoids, 42% for monohydroxy-containing eicosanoids, and 50% for PUFAs. The settings for data-dependent scan MS/MS were as follows: isolation width, m/z 1.5; normalized collision energy, 40%; minimum signal required, 100,000; minimum MSⁿ signal required, 10,000; repeat count, 3; repeat duration, 0.5 min; exclusion duration, 1.5 min. Automated gain control was set at $\sim 2 \times 10^7$ for MS and MS/MS full scan.

Deuterium-labeled PGE₂ (d_7 -PGE₂), d_7 -LTB₄, and d_{19} -PUFA were routinely used in our laboratory as the internal standard to calculate recoveries during sample preparation and quantification. Deuterium-labeled eicosanoids were also routinely used to calibrate CRTs and account for potential daily variations in relative chromatographic behavior. CRTs for LMs were routinely within \pm 0.6 min.

Generation of eicosanoids by polymorphonuclear leukocytes and stimulated spleen

Results from LC-UV-MS/MS for eicosanoids acquired from biological samples were used to demonstrate the performance of the databases and algorithms constructed. One sample set was obtained by incubations of rabbit polymorphonuclear leukocytes ($\sim 50 \times 10^6$ cells per incubation) isolated from rabbit whole blood and stimulated with ionophore A23187 (15 μ M) and arachidonic acid (10 μ M, 20 min, 37°C) as described (19). Samples were also analyzed from murine spleens (kindly provided by J. Aliberti and coworkers) prepared as described (20). The spleens were collected from mice injected with homogenate of *Toxoplasma gondii* (RH strain). Incubation of samples was stopped with two volumes of methanol, and samples were maintained at –20°C before isolation and further analyses. All samples were extracted using a solid-phase extraction technique (21). In short, samples rapidly preequilibrated at pH 3.5 were loaded onto solid-phase extraction cartridges (100 mg of C18 adsorbent per cartridge; Varian, Palo Alto, CA) and eluted with 8 ml of methyl formate (EM Science, Gibbstown, NJ). Samples were taken to dryness using a flow of nitrogen gas. Each sample was suspended in 20 μ l of mobile phase C and injected for LC-UV-MS/MS analysis.

Software

For LMs and related compounds for which synthetic and authentic standards were available, the databases were constructed with MassFrontier (version 2.0; HighChem, Ltd., San Jose, CA) (22), a commercial software designed for use with positive-ion MS spectra generated by electron impact ionization. We implemented cognitive-contrast-angle and theoretical algorithms and developed databases using Microsoft Visual Studio 6.0 for

mass spectra obtained in the negative-ion mode. All of the spectra generated were processed with Microsoft Excel 2000.

Tests to evaluate and optimize systems of LC-UV-MS/MS mediator-lipidomic databases and algorithms

Murine tissue was extracted along with different amounts of LMs, their precursors, and metabolites that were added for these experiments. Each of six different murine tissues (kidney, spleen, liver, brain, colon, and fat) was homogenized in cold methanol. Each homogenate was centrifuged (14,000 rpm, 20 min), and supernatants were spiked with 1, 2.5, or 5 ng of the following 34 LMs and the related compounds denoted in **Table 1** ($n = 2-3$). The trihydroxy-containing eicosanoids LXA₄, LXB₄, 5*S*,12*R*,20-trihydroxy-6*E*,8*Z*,10*E*,14*Z*-eicosatetraenoic acid; the dihydroxy-containing eicosanoids 5,15-diHETE (5,15-dihydroxy-6*E*,8*E*,11*Z*,13*Z*-eicosatetraenoic acid), LTB₄, 5*S*,6*S*-diHETE (5*S*,6*S*-dihydroxy-7*E*,9*E*,11*Z*,14*Z*-eicosatetraenoic acid), 5*S*,6*R*-diHETE (5*S*,6*R*-dihydroxy-7*E*,9*E*,11*Z*,14*Z*-eicosatetraenoic acid), 12*S*,20-dihydroxyeicosa-5*Z*,8*Z*,10*E*,14*Z*-tetraenoic acid; HETEs (monohydroxy eicosatetraenoic acids), 20-HETE (20-hydroxy-5*Z*,8*Z*,11*Z*,14*Z*-eicosatetraenoic acid), 15*S*-HETE (15*S*-hydroxy-5*E*,8*Z*,11*Z*,13*Z*-eicosatetraenoic acid), 12*S*-HETE (12*S*-hydroxy-5*Z*,8*Z*,10*E*,14*Z*-eicosatetraenoic acid), 11-HETE (11-hydroxy-5*E*,8*Z*,12*Z*,14*Z*-eicosatetraenoic acid), 8-HETE (8-hydroxy-5*E*,9*Z*,11*Z*,14*Z*-eicosatetraenoic acid), and 5*S*-HETE (5*S*-hydroxy-6*E*,8*Z*,11*Z*,14*Z*-eicosatetraenoic acid); the prostaglandin PGE₂, 9-oxo-11*α*,15*S*-dihydroxy-prost-13*E*-en-1-oic acid, 9,15-dioxo-11*α*-hydroxy-prosta-5*Z*,13*E*-dien-1-oic acid, 9,15-dioxo-11*α*-hydroxy-prost-5*Z*-en-1-oic acid, 9*α*,15*S*-dihydroxy-11-oxo-prosta-5*Z*,13*E*-dien-1-oic acid, PGF_{2α}, 9,15-dioxo-11*α*-hydroxy-prosta-13*E*-en-1-oic acid, 6-oxo-9*α*,11*α*,15*S*-trihydroxy-prost-13-en-1-oic acid, 11-oxo-prosta-5*Z*,9,12*E*,14*Z*-tetraen-1-oic acid, 15*S*-hydroxy-11-oxo-

prosta-5*Z*,9*E*,13*E*-trien-1-oic acid, and 9*α*-hydroxy-11-oxo-prosta-5*Z*,12*E*,14*E*-trien-1-oic acid; the precursors of LMs arachidonic acid (eicosa-5*Z*,8*Z*,11*Z*,14*Z*-tetraenoic acid), eicosapentaenoic acid [eicosa-5*Z*,8*Z*,11*Z*,14*Z*,17*Z*-pentaenoic acid (20:5,n-3)], docosahexaenoic acid [docosa-4*Z*,7*Z*,10*Z*,13*Z*,16*Z*,19*Z*-hexaenoic acid (22:6,n-3)], and linolenic acid [octadeca-9*Z*,12*Z*,15*Z*-trienoic acid (18:3,n-3)]; and others: 15-oxo-eicosa-5*Z*,8*Z*,11*Z*,13*E*-tetraenoic acid, 5*S*-hydroxy-6*R*-(*S*-glutathionyl)-7*E*,9*E*,11*Z*,14*Z*-eicosatetraenoic acid, 5*S*-hydroxy-6*R*-(*S*-cysteinylglycyl)-7*E*,9*E*,11*Z*,14*Z*-eicosatetraenoic acid, 9*α*,11,15*S*-trihydroxythromba-5*Z*,13*E*-dien-1-oic acid, and heptoxilin A₃ [8(*R,S*)-hydroxy-11*S*,12*S*-epoxy-eicosa-5*Z*,9*E*,14*Z*-trienoic acid]. Each sample was then concentrated by a stream of N₂ gas, dissolved into 20 μ l of mobile phase C, and injected into the instrument to acquire LC-UV-MS/MS chromatograms and spectra, which were then searched against the databases using the algorithms that we developed (vide infra). For each amount of one compound in six different tissues, one value of percentage correct for best match was obtained. The mean and SEM of percentage correct for best match were calculated from one compound group at one amount for each database/algorithm. The primary measure of performance in these experiments was the correct best match and compound identification.

RESULTS AND DISCUSSION

Logic diagram used to identify and elucidate structures of LMs with mediator-lipidomic databases and algorithms

The regular routes for LM identification and structure elucidation of potentially novel LMs were followed in the

TABLE 1. Percentage correct for best match to identify LMs and their precursors and metabolites in murine tissue and organ samples using mediator-lipidomic liquid chromatography-ultraviolet-tandem mass spectrometry databases and algorithms

Database and Algorithm	LMs, Their Precursors, or Metabolites	Percentage Correct for Best Match		
		1 ng	2.5 ng	5 ng
Cognoscitive-contrast-angle algorithm and databases	Monohydroxy-containing eicosanoids	100.0 \pm 0.0	100.0 \pm 0.0	93.3 \pm 11.5
	Dihydroxy-containing eicosanoids	100.0 \pm 0.0	100.0 \pm 0.0	100.0 \pm 0.0
	Trihydroxy-containing eicosanoids	100.0 \pm 0.0	100.0 \pm 0.0	100.0 \pm 0.0
MassFrontier	Arachidonic acid, eicosapentaenoic acid, docosahexaenoic acid, and linolenic acid	100.0 \pm 0.0	100.0 \pm 0.0	100.0 \pm 0.0
	Monohydroxy-containing eicosanoids	73.3 \pm 19.0	100.0 \pm 0.0	80.0 \pm 10.0
	Dihydroxy-containing eicosanoids	100.0 \pm 0.0	100.0 \pm 0.0	100.0 \pm 0.0
	Trihydroxy-containing eicosanoids	100.0 \pm 0.0	100.0 \pm 0.0	100.0 \pm 0.0
	Prostaglandin	87.6 \pm 14.4	93.3 \pm 12.7	89.9 \pm 10.4
	15-oxo-EETE, LTC ₄ , LTD ₄ , TXB ₂ , and heptoxilin A ₃	100.0 \pm 0.0	100.0 \pm 0.0	100.0 \pm 0.0
Theoretical	Monohydroxy-containing eicosanoids	80.5 \pm 10.9	88.4 \pm 12.6	93.3 \pm 6.5
	Dihydroxy-containing eicosanoids	95.4 \pm 12.3	97.1 \pm 8.2	100.0 \pm 0.0
	Trihydroxy-containing eicosanoids	100.0 \pm 0.0	100.0 \pm 0.0	88.9 \pm 19.2

Values shown are means \pm SEM. LM, lipid mediator. Each of the six different murine tissues or organs (kidney, spleen, liver, brain, colon, and fat) was homogenized in cold methanol. Each homogenate was centrifuged, and supernatants were simultaneously spiked with 1, 2.5, or 5 ng of 34 LMs and the related compounds ($n = 2-3$). These included the trihydroxy-containing eicosanoids 5*S*,6*R*,15*S*-trihydroxy-7*E*,9*E*,11*Z*,13*E*-trans-11-*cis*-eicosatetraenoic acid, 5*S*,14*R*,15*S*-trihydroxy-6*E*,8*Z*,10*E*,12*E*-eicosatetraenoic acid, and 5*S*,12*R*,20-trihydroxy-6*E*,8*Z*,10*E*,14*Z*-eicosatetraenoic acid; the dihydroxy-containing eicosanoids 5,15-diHETE (dihydroxy-eicosatetraenoic acids), LTB₄, 5*S*,6*S*-diHETE, 5*S*,6*R*-diHETE, and 12*S*,20-dihydroxyeicosa-5*Z*,8*Z*,10*E*,14*Z*-tetraenoic acid; the HETEs (monohydroxy eicosatetraenoic acids) 20-HETE, 15*S*-HETE, 12*S*-HETE, 11-HETE, 8-HETE, and 5*S*-HETE; the prostaglandin 11*α*,15*S*-dihydroxy-9-oxo-prosta-5*Z*,13*E*-dien-1-oic acid, 9-oxo-11*α*,15*S*-dihydroxy-prost-13*E*-en-1-oic acid, 9,15-dioxo-11*α*-hydroxy-prosta-5*Z*,13*E*-dien-1-oic acid, 9,15-dioxo-11*α*-hydroxy-prost-5*Z*-en-1-oic acid, 9*α*,15*S*-dihydroxy-11-oxo-prosta-5*Z*,13*E*-dien-1-oic acid, 9*α*,11*α*,15*S*-trihydroxy-prosta-5*Z*,13*E*-dien-1-oic acid, 9,15-dioxo-11*α*-hydroxy-prosta-13*E*-en-1-oic acid, 6-oxo-9*α*,11*α*,15*S*-trihydroxy-prost-13-en-1-oic acid, 11-oxo-prosta-5*Z*,9,12*E*,14*Z*-tetraen-1-oic acid, 15*S*-hydroxy-11-oxo-prosta-5*Z*,9*E*,13*E*-trien-1-oic acid, and 9*α*-hydroxy-11-oxo-prosta-5*Z*,12*E*,14*E*-trien-1-oic acid; the LM precursors arachidonic acid, eicosapentaenoic acid, docosahexaenoic acid, and linolenic acid; and others: 15-oxo-EETE (15-oxo-5*Z*,8*Z*,11*Z*,13*E*-eicosatetraenoic acid), LTC₄ [5*S*-hydroxy-6*R*-(*S*-glutathionyl)-7*E*,9*E*,11*Z*,14*Z*-eicosatetraenoic acid], LTD₄ [5*S*-hydroxy-6*R*-(*S*-cysteinylglycyl)-7*E*,9*E*,11*Z*,14*Z*-eicosatetraenoic acid], TXB₂ (9*α*,11,15*S*-trihydroxythromba-5*Z*,13*E*-dien-1-oic acid), and heptoxilin A₃. For each amount of one compound in six different tissues, one value of percentage correct for best match was obtained. The mean and SEM of percentage correct for best match were calculated from one compound group at one amount for each of the three databases/algorithms (see Systems and Methodology for details).

mediator-lipidomic databases and search algorithms that we constructed (**Scheme 2**). Two types of lipidomic databases for LMs were used for searching: one contains LC-UV-MS/MS spectra and chromatograms acquired on LM standards, and the other is based on theoretically generated LC-UV-MS/MS spectra and chromatograms. The searches were conducted stepwise against either standards or the theoretical databases to increase the search speed. The search of MS/MS spectra was carried out only against the MS/MS subdatabase with the molecular ion of interest (i.e., M-1) and matched UV spectra (e.g., conjugated diene, triene, or tetraene chromophores). Subsequently, the matching of CRTs was performed. The standard error for CRTs for the chromatographic conditions used in the present set of experiments was ~ 0.3 min. Thus, only the unknown CRT within $\pm 2 \times 0.3$ min of the CRT (for 95% confidence intervals) in the databases was taken as a correct match. If the UV spectral pattern was unclear, the MS/MS and CRT were still searched to avoid potential errors in assignment. A standard LM or theoretical fragmentation/ion fragmentation pattern that fulfilled the above match criteria was then assigned to the unknown set. If the match was a "hit" only with UV and MS/MS spectra but not with CRT, the LM in the sample was likely to be a geometric isomer of a known LM.

UV patterns are simply presented in the database as λ_{\max} and divided into six clusters: ~ 301 nm, ~ 278 nm, ~ 270 nm, ~ 242 nm, ~ 235 nm, and vacuum UV. In contrast, each MS/MS spectrum has dozens of ions and therefore is a much larger data set than a UV λ_{\max} . If the UV λ_{\max} is matched first, then only the MS/MS subdatabase having LM standards with this UV λ_{\max} , which is a fraction of the whole MS/MS database, needs to be searched. This type of narrowed search is faster than that through the entire MS/MS database. This will become more significant when more and more standard MS/MS data are entered into the database. We tested the route with MS/MS spectra before UV; the search results are the same as having MS/MS after UV data. If the UV pattern is unclear, we can

just search the MS/MS and CRT to avoid the assignment errors.

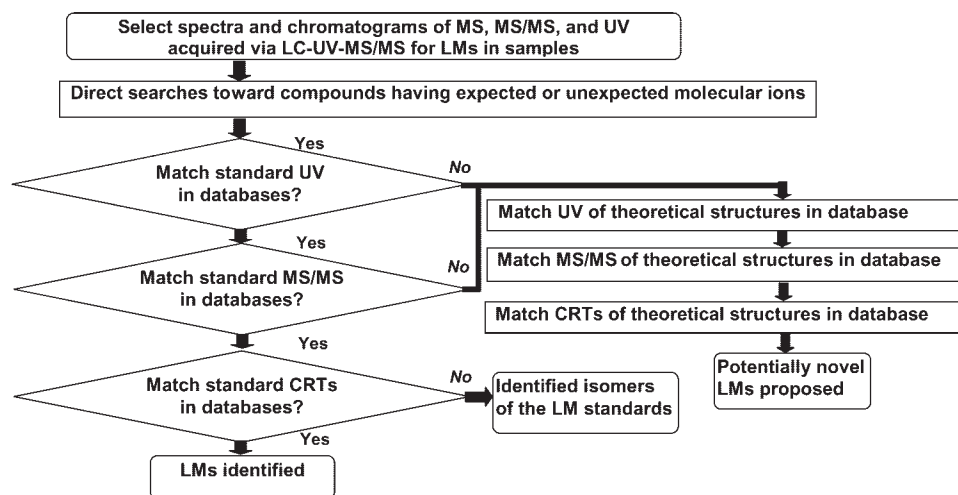
Databases constructed with commercial mass spectral software containing LC-UV-MS/MS chromatograms and spectra measured from standard LMs

A mediator-lipidomic database using LC-UV-MS/MS spectra and chromatograms acquired from authentic LMs was constructed with GC-MS spectral software MassFrontier. The UV λ_{\max} of standard LMs were written into the subdatabase names and the CRTs were written into the LM names, so that MassFrontier could handle the acquired UV spectral results and CRTs for the identification of the unknown LMs according to the logic diagram in Scheme 2.

The demonstration of the efficacy of this database was assessed with the identification of eicosanoids biosynthesized by rabbit leukocytes using LC-UV-MS/MS (**Fig. 1**). For peak I in the inset of **Fig. 1A**, a subdatabase "mTOz 351Vacuum UV" was selected with the molecular ion of interest and matched UV λ_{\max} . The search showed that the MS/MS spectrum of peak I matched best with PGE₂, with the highest matching score of 907 (**Fig. 1B**). Furthermore, the CRT of peak I and standard PGE₂ matched. Therefore, peak I was assigned as PGE₂, consistent with the manual identification and assessment of MS and UV spectral and LC chromatographic features of PGE₂.

COCAD: using MS/MS ion identities and intensities as well as UV spectra and CRTs for LM identification

Identification of mass spectral ions generated from LMs. The system with COCAD that we developed can be used to elucidate the fragmentation of LMs in mass spectrometry and to match unknown MS/MS spectra with those of synthetic and/or authentic standards. In the process of matching, the intensity of each peak is treated differently based on the ion identity. MS/MS ions are clustered into three types: "peripheral-cut" ions, formed by neutral loss of water, CO₂, amino acid, or amines derived from functional groups linking to the LM carbon chain as hydroxy, hydro-



Scheme 2. Logic diagram for developing LC-UV-MS/MS-based mediator-lipidomic databases and search algorithms for PUFA-derived lipid mediators (LMs). CRT, chromatographic retention time.

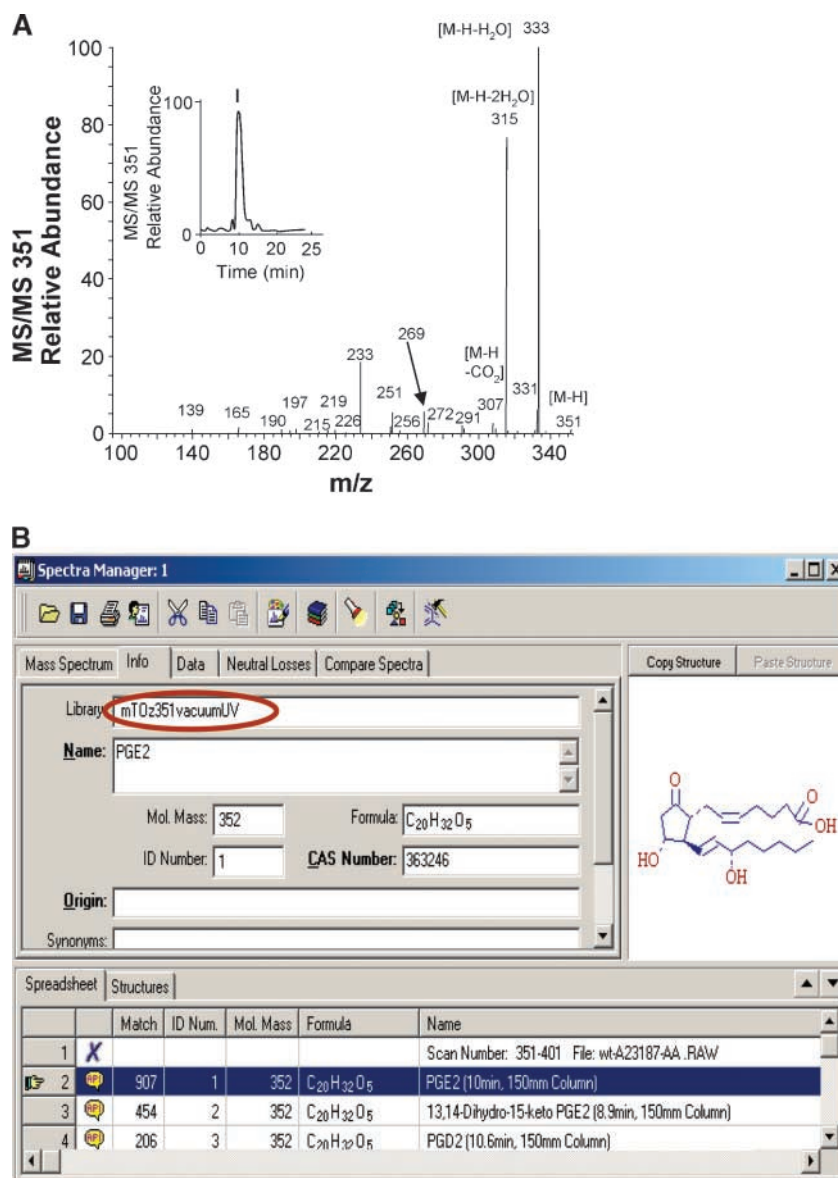
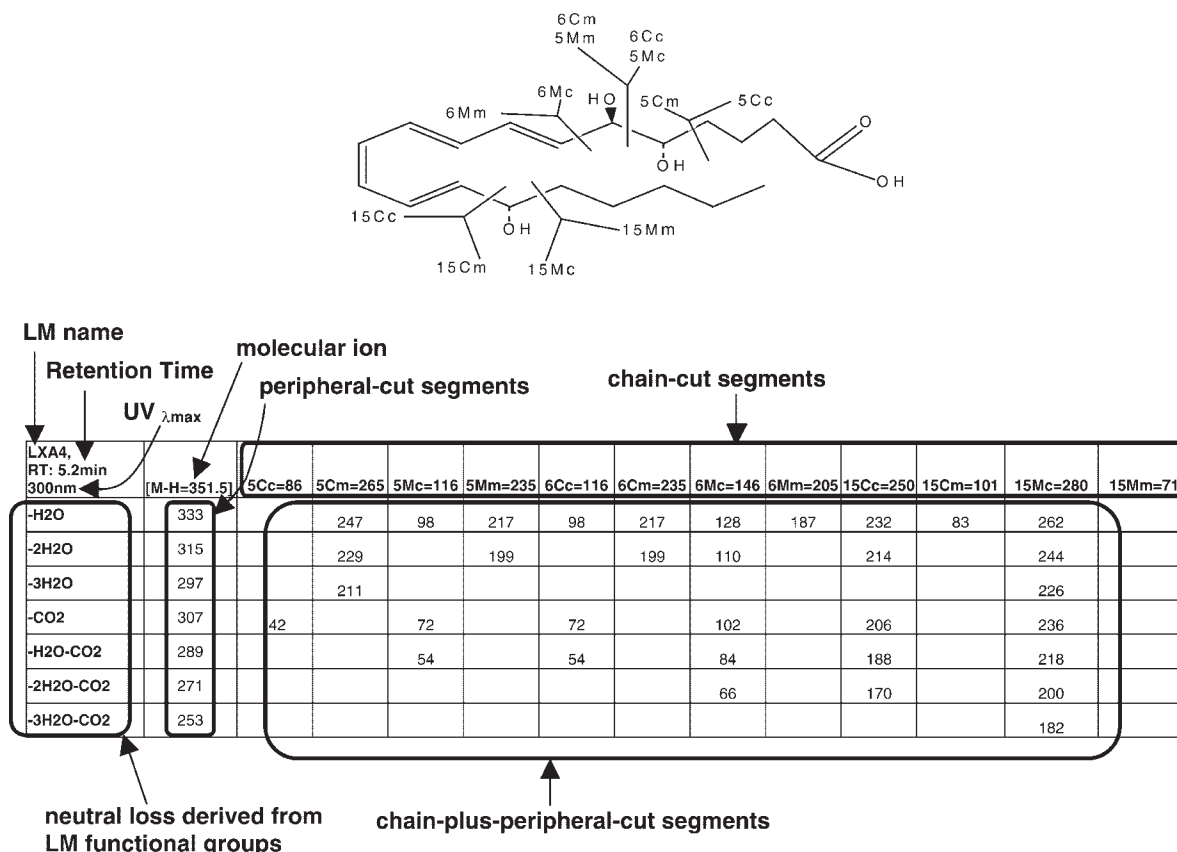


Fig. 1. Identification of 11 α ,15 β -dihydroxy-9-oxo-prosta-5 Z ,13 E -dien-1-oic acid (PGE₂) generated by rabbit leukocytes using a mediator-lipidomic database and algorithm developed with MassFrontier. A: MS/MS spectrum, and MS/MS of m/z 351 chromatogram (inset) were acquired for PGE₂ generated from incubation of rabbit polymorphonuclear leukocytes and arachidonic acid (representative; $n = 3$). The MS/MS scan conditions were as follows: parent ion, m/z 351; isolation width, 1.5; normalized collision energy, 42%; activation time, 30 ms; scan of MS/MS ions, from m/z 95 to 355. The LC column used was 150 mm long, 2 mm inner diameter, and packed with 5 μ m of C18 particles. The gradient for the mobile phase is described in Systems and Methodology. B: Report for the search via the MassFrontier system showing PGE₂ as the best match.

peroxy, carbonyl, epoxy, carboxy, amino acid group, or amino group; “chain-cut” ions, formed by the cleavage of a carbon-carbon bond along the LM carbon chain; and “chain-plus-peripheral-cut” ions, formed by a combination of chain cut and peripheral cut. Molecular ions formed during ESI can easily be converted to peripheral-cut ions in the MS/MS process. Similarly, chain-cut ions can also be readily converted to chain-plus-peripheral-cut ions (Scheme 3).

Typical chain-cut ions for LMs in MS/MS are formed by α -cleavage of the carbon-carbon bonds connecting to the carbon with a functional group directly attached (2–4, 7,

8). LMs readily undergo α -cleavage (7). We proposed the nomenclatures illustrated in the LXA₄ structure presented in Scheme 3 to systematically name the segments formed via chain cut and chain plus peripheral cut without concern for hydrogen shifts occurring during mass spectrometric analysis of PUFA-derived products. Each of these LMs derived from PUFA has a carboxyl terminus and a methyl terminus. An Arabic number was used to designate the position of the functional group on the LM carbon chain where the cleavage occurs. The uppercase letter right after the number indicates the side of the functional group on which the cleavage occurs: C is for



Scheme 3. LC-UV-MS/MS database layout: example for naming LM segments. In this case, the example shown is lipoxin A₄ (LXA₄), formed via chain cut, peripheral cut, and chain plus peripheral cut for interpretation of MS/MS fragmentation. RT, retention time.

cleavage on the carboxyl side of the functional group, and M is for cleavage on the methyl side of the functional group. Each cleavage can directly generate two segments. The lowercase letter that follows indicates the side of the cleavage on which the segment forms: c is for a segment formed on the carboxyl side of the cleavage, and m is for a segment formed on the methyl side of the cleavage. Segments formed through β -cleavage or γ -cleavage toward the functional group are named by adding β or γ between the uppercase and lowercase letters. Because three hydroxy groups of LXA₄ are located at C₅, C₆, and C₁₅ of the 20 carbon linear chain, α -cleavages can occur on the bonds at C₄-C₅, C₅-C₆, C₆-C₇, C₁₄-C₁₅, and C₁₅-C₁₆ to generate 10 chain-cut segments (Scheme 3). All of the possible chain-cut, peripheral-cut, and chain-plus-peripheral-cut segments for LXA₄ are listed in the table in Scheme 3.

A MS/MS ion detected from LM samples in the negative-ion mode generally is formed from a specific segment with the addition or subtraction of hydrogen(s) caused by hydrogen shift during the cleavage. The charge (*z*) of the LM negative ion is usually equal to 1; therefore, the mass-to-charge ratio (*m/z*) of a LM ion is usually equal to its mass (*m*). Previous reports (7, 8, 11) and our unpublished results (data not shown) demonstrated that the MS/MS fragmentation observes the empirical rules regarding the addition or subtraction of hydrogen(s) for the chain-cut segments to form the chain-cut MS/MS ions: for segment

Cc, the detected MS/MS ions are Cc and Cc + H; for segment Cm, the detected MS/MS ions are Cm, Cm \pm H, and Cm \pm 2H; for segment Mc, the detected MS/MS ions are Mc and Mc - H; and for segment Mm, the detected MS/MS ions are Mm, Mm \pm H, and Mm \pm 2H (referred to below as the fragmentation rules).

These rules were used to identify the segments for instrument-detected MS/MS ions. The interpreted ions, such as M - H - H₂O, Cc, Cc + H, and Mc - H, identified as the MS/MS ions detected in the mass spectrometer, are called virtual ions. One detected MS/MS ion can be interpreted as one or several virtual ions. Through the loss of H₂O, CO₂, NH₃, and/or amino acids, the chain-cut ions can form chain-plus-peripheral-cut ions. For the chain-cut and chain-plus-peripheral-cut ions in the present report, we focused on those formed by α -cleavages. Those detected MS/MS ions uninterpretable via rule 1 and neutral loss are taken as unidentified ions.

Modification of MS/MS ion intensities according to their identities. In nature, isotope ¹³C constitutes 1.1% of elemental carbon. If the intensity of an ion with mass *M* (ion charge *z* is 1) containing only carbons, hydrogens, and oxygen(s) is 100, the contribution of ¹³C to the intensity of the ion with mass (*M* + 1) (the ion with mass 1 unit higher) is statistically equal to 100 \times 1.1% \times the number of carbons in ion *M*, which is listed in Table 2.2 of the report by McLafferty and Turecek (23). The contribution of ¹³C to the ion (*M* + 2)

is much less than $100 \times 1.1\% \times \text{carbon number}$. The ^{13}C contribution of ion M to the intensities of ions $(M + 1)$ and $(M + 2)$ was subtracted in the computation of the matching score for the COCAD and theoretical algorithms. If ion M could not be identified, the carbon number in the ion $(M + 1)$ or $(M + 2)$ is used because M , $(M + 1)$, and $(M + 2)$ generally have the same carbon number.

Chain-cut ions are most informative and can be diagnostic for determining LM structures such as the position of functional groups and double bonds. Generally, there are more chain-plus-peripheral-cut ions than chain-cut ions, because the former are derived from the latter by one or several neutral losses. It is likely that some chain-plus-peripheral-cut ions have the same m/z even though they originate by different mechanisms and represent different structural features. Therefore, chain-cut ions are more specific than chain-plus-peripheral-cut ions for defining the LM structure. Peripheral-cut ions in MS/MS spectra are similar among LM isomers; therefore, they were not specific enough for differentiation of individual LM isomers.

According to the fragmentation rules, the n th MS/MS peak can be identified as one or several chain-cut (C) ions, peripheral-cut (P) ions, and/or chain-plus-peripheral-cut (CP) ions. The weighted intensity (I_n') of each identified ion is as follows:

$$I_n' = I_n \div (C_n M + CP_n M + P_n M \times \rho) \times W \quad (\text{Eq. 1})$$

where y is the MS/MS ion type identified as C , P , or CP ; I_n' is the relative intensity of the n th peak in the MS/MS spectrum;

$$C_n M$$

is the number of chain-cut ions identified for the n th MS/MS peak;

$$CP_n M$$

is the number of chain-plus-peripheral-cut ions identified for the n th MS/MS peak;

$$P_n M$$

is the number of peripheral-cut ions identified for the n th MS/MS peak; and W is the weight measuring the importance of the identified ion to determine the LM structure. It is 10 as CW and 1 as CPW or PW . The fingerprint features of chain-cut ions are used to define LM structure by multiplying their intensities by 10, which was determined to be the best among the values (2, 10, 20, and 100) tested. Weighted MS/MS ion intensities are used for COCAD and the theoretical system described below. ρ represents the contribution of peripheral-cut ions to I_n' ($\rho = 3$ for peripheral-cut ions formed via the loss of one CO_2 from each molecular ion, $\rho = 10$ for peripheral-cut ions formed via the loss of one H_2O from each molecular ion, and $\rho = 1$ for other peripheral-cut ions formed via multiple loss of CO_2 and/or H_2O from each molecular ion). The assignment of ρ values is arbitrary and based on the observation of relative intensities of peripheral-cut ions in MS/MS spectra of LMs.

COCAD contrast angle. COCAD used a contrast-angle algorithm to match an MS/MS spectrum between sample and standards. The contrast angle is calculated as follows:

$$C_v = \sum_{n=1}^N (C_n B_v \times C_n I_n) \quad (\text{Eq. 2})$$

$$CP_v = \sum_{n=1}^N (CP_n B_v \times CP_n I_n) \quad (\text{Eq. 3})$$

$$P_v = \sum_{n=1}^N (P_n B_v \times P_n I_n) \quad (\text{Eq. 4})$$

$$D_C(D_{CP}, \text{ or } D_P) = \frac{\sum_{v=1}^V U_v S_v}{\sqrt{\sum_{v=1}^V U_v^2 \sum_{v=1}^V S_v^2}} \quad (\text{Eq. 5})$$

U_v is equal to C_v , CP_v , or P_v for unknown spectrum to be identified; S_v is equal to C_v , CP_v , or P_v for standard spectrum.

$$\text{COCAD contrast angle} = \quad (\text{Eq. 6})$$

$$\cos^{-1}[(10 \times D_C + D_P + D_{CP}) \div (11 + \omega_{CP})]$$

where v is the v th virtual ion and V is the total number for one type of virtual ion formed via chain cut, chain plus peripheral cut, or peripheral cut for a specific LM.

$$C_n B_v$$

is equal to 1 if the n th MS/MS peak can be identified as the v th virtual ion formed via chain cut and is equal to 0 if not;

$$CP_n B_v$$

or

$$P_n B_v$$

has a similar meaning but for ions formed via chain plus peripheral cut or peripheral cut; N is the total number of peaks in the MS/MS spectrum. D_C is the dot-product between the virtual vectors of U (unknown sample) and S (standard) formed via chain cut; D_{CP} and D_P are the dot-products for chain-plus-peripheral-cut and peripheral-cut ions, respectively. D_C , D_{CP} , or D_P in equation 5 represents the similarity of ions formed via chain cut, chain plus peripheral cut, or peripheral cut between an unknown spectrum and a standard spectrum. None of them is greater than 1. The v th virtual ion is not used for the calculation of the corresponding D_C , D_{CP} , or D_P if either U_v or S_v is 0. If every C_v , CP_v , or P_v within the vectors is 0, then D_C , D_{CP} , or D_P , respectively, is assigned the value 0.

The COCAD contrast angle in equation 6 represents how well the spectrum of the sample matches the standard: if it is 0° , the two spectra match exactly; if it is 90° , the two spectra do not match at all. The smaller the contrast angle between 0° and 90° , the better the match (13, 24). The value is integrated and normalized from dot-products D_C , D_{CP} , and D_P (equation 6). The numeric coef-

efficient 10 in equation 6 was found to be the best value (2, 20, and 100 were also tested) that emphasizes the fingerprinting feature of chain-cut ions, because chain-cut ions are more important for determining the LM structure than are other types of ions. To normalize $[(10 \times D_C + D_{CP} + D_P) \div (11 + \omega_{CP})]$ in equation 6 to be no more than 1, 11 was used in the denominator of equation 6, and ω_{CP} is equal to 1 if at least one MS/MS ion is identified as a chain-plus-peripheral-cut virtual ion or is equal to 0 if no such ion is identified. No chain-plus-peripheral-cut ion is identified in a few LM standard spectra. Therefore, ω_{CP} is introduced in equation 6 to normalize the COCAD contrast angle to 0 when matching these types of spectra against themselves. Unidentified ions were excluded for matching in equations 2 to 6.

According to the empirical fragmentation rules, for monohydroxy-containing LMs, the ν th chain-cut ion can be Cc, Cc + 1, Cm - 2, Cm - 1, Cm, Cm + 1, Cm + 2, Mc - 1, Mc, Mm - 2, Mm - 1, Mm, Mm + 1, or Mm + 2. The ν th chain-plus-peripheral-cut ion can be Cc - CO₂, Cc - CO₂ + 1, Cm - H₂O - 2, Cm - H₂O - 1, Cm - H₂O, Cm - H₂O + 1, Cm - H₂O + 2, Mc - H₂O - 1, Mc - H₂O, Mc - CO₂ - 1, Mc - CO₂, Mc - H₂O - CO₂ - 1, or Mc - H₂O - CO₂. The ν th peripheral-cut ion can be M - H - CO₂, M - H - H₂O, or M - H - H₂O - CO₂. For LMs having multiple functional groups, V is accordingly greater.

Integrating MS/MS spectra with UV spectra and chromatograms in COCAD to identify LMs. COCAD databases incorporate the LC-UV-MS/MS chromatograms and spectra measured from standard LMs and the segments formed by cleavage illustrated in Scheme 3. The features of UV spectra and chromatograms are represented with the UV λ_{\max} and CRTs, respectively. The search of COCAD databases was conducted stepwise, as depicted in the logical diagram shown in Scheme 2, from UV λ_{\max} , to MS/MS spectra, and then to CRTs. Using COCAD, we identified LXA₄ in murine spleen stimulated during exposure to *T. gondii* (Fig. 2A, B). The search was narrowed to the subdatabase with UV λ_{\max} 301 nm (Fig. 2A, middle inset) and molecular ion m/z 351, which were detected for the unknown peak II in the chromatogram (m/z 251 of MS/MS 351) for the stimulated spleen sample. The CRT (5.2 min) of peak II was then matched against the candidates with the highest MS/MS match scores (Fig. 2A, left inset). For comparison, searching was also conducted with the system developed with MassFrontier (Fig. 2C). Both demonstrated that LXA₄ was the best match for the unknown peak II shown in Fig. 2A. However, COCAD and MassFrontier could not be used alone to identify the structures of unknowns without LC-UV-MS/MS chromatograms and spectra obtained for authentic and/or synthetic standards.

Theoretical database and search algorithm for identification of potentially novel LMs

Theoretical databases consist of the segments (Scheme 3), the UV λ_{\max} , and CRTs predicted for potentially novel LMs. Searching against a theoretical database is also performed stepwise as described in Scheme 2, from UV λ_{\max} , to MS/MS spectra, and then to CRTs.

Equation 7 is the matching score for an unknown MS/MS spectrum compared with the virtual spectrum based on the segments and the fragmentation rules.

$$\text{Matching score} = \left\{ \sum_{f=1}^F \left[\sum_{n=1}^N (C_{I_n} \times C_f M_n) \times (fT_C \div fA_C)^{0.5} \right] + \sum_{f=1}^F \left[\sum_{n=1}^N (C_{I_n}^{CP} \times C_f M_n) \times (fT_{CP} \div fA_{CP})^{0.5} \right] + \sum_{n=1}^N [P_{I_n} \times P M_n \times (T_P \div A_P)^{0.5}] \right\} \div \sum_{n=1}^N (C_{I_n} + C_{I_n}^{CP} + P_{I_n}) \quad (\text{Eq. 7})$$

The matching score in equation 7 summates the weighted intensities of all of the identified MS/MS peaks in the spectrum acquired from the sample. The numerator of the formula is composed of three parts:

$$\sum_{f=1}^F \left[\sum_{n=1}^N (C_{I_n} \times C_f M_n) \times (fT_C \div fA_C)^{0.5} \right]$$

summing the weighted intensities of MS/MS peaks identified as chain-cut ions;

$$\sum_{f=1}^F \left[\sum_{n=1}^N (C_{I_n}^{CP} \times C_f M_n) \times (fT_{CP} \div fA_{CP})^{0.5} \right]$$

summing the weighted intensities of MS/MS peaks identified as the chain-plus-peripheral-cut ions; and

$$\sum_{n=1}^N [P_{I_n} \times P M_n \times (T_P \div A_P)^{0.5}]$$

summing the weighted intensities of MS/MS peaks identified as the peripheral-cut ions.

$$C_f M_n$$

is the total number of chain-cut ions via α -cleavage formed from the f th functional group and matched to the n th MS/MS peak. F is the total number of functional groups in one LM. f is counted from the carboxyl terminus of LM. For example, f is 1 for the 5-hydroxy, 2 for the 6-hydroxy, and 3 for the 15-hydroxy group present in LXA₄. F for LXA₄ is 3 (Scheme 3).

$$\sum_{n=1}^N (C_{I_n} \times C_f M_n)$$

summates the weighted intensities of MS/MS peaks identified as chain-cut ions formed from the f th functional group via α -cleavage. The smallest MS/MS ion detectable in ion trap tandem mass spectrometry is generally $\sim m/z$ 95 for LMs with a molecular ion of ~ 400 Da (25). To compensate for the bias caused by the inability to detect an MS/MS ion of $m/z < 95$, factors $(fT_C \div fA_C)^{0.5}$, $(fT_{CP} \div fA_{CP})^{0.5}$, and $(T_P \div A_P)^{0.5}$ are used in equation 7. fT_C (or fT_{CP}) is the total number of chain-cut (or chain-plus-peripheral-cut) ions formed from the f th functional group via α -cleavage. T_P is the total number of peripheral-cut ions formed from one LM. fA_C (fA_{CP} or A_P) is the fraction of fT_C (fT_{CP} or T_P) representing the ions within the MS/MS

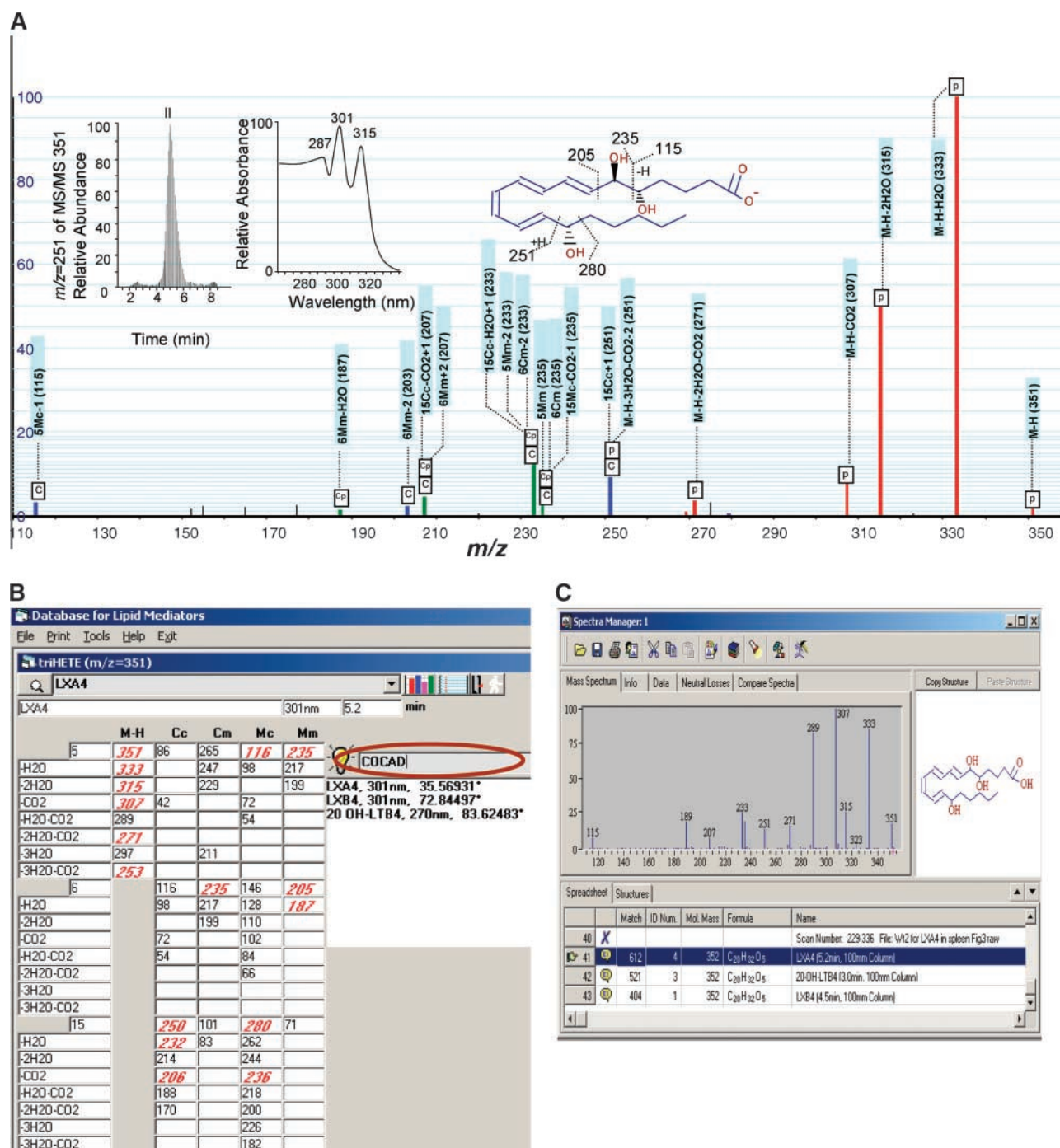


Fig. 2. Cognitive-contrast-angle algorithm and databases (COCAD)-based identification of 5*S*,6*R*,15*S*-trihydroxy-7*E*,9*E*,11*Z*,13*E*-*trans*-11-*cis*-eicosatetraenoic acid (LXA₄) in murine spleens. Mice were exposed to *T. gondii* as described previously (20). Here, we used COCAD that we developed (representative; $n = 3$). A: Identification, interpretation, and annotation of anions in a MS/MS (at m/z 351) spectrum. The MS/MS scan conditions were as follows: parent ion, m/z 351; isolation width, 1.5; normalized collision energy, 35%; activation time, 30 ms; scan of MS/MS ions, from m/z 95 to 355. C, chain-cut ion; Cp, chain-plus-peripheral-cut ion; P, peripheral-cut ion. The insets are chromatogram (at m/z 251 of MS/MS 351; left), UV spectrum (middle), and proposed MS/MS segments on LXA₄ (right). The chromatogram at m/z 251 of MS/MS 351 was the intensity temporary profile or extracted chromatogram for ion m/z 251 in the MS/MS spectrum of parent ion m/z 351 generated by electrospray ionization (ESI). B: Report shows that LXA₄ was identified as the best match for the LC-UV-MS/MS data in the COCAD system (with highest match score). C: LXA₄ was also identified by searching the database constructed by MassFrontier. The LC column used was 100 mm long (see details in Systems and Methodology).

detecting range (m/z from 95 to the m/z of molecular ion). 20-HETE is a typical example. The ions formed from the segment 20Cm and 20Cm - H₂O of 20-HETE are m/z 31 and 13 according to the fragmentation rules, which are too

small to be detected in ion trap MS/MS. Consequently, without the use of factors ($I_{TC} \div I_{AC}$)^{0.5} and ($I_{TCP} \div I_{ACP}$)^{0.5}, 20-HETE could have a lower matching score than other HETEs, even though the MS/MS spectrum is that of 20-HETE.

$$\sum_{n=1}^N (C_{I_n} + {}^{CP}I_n + P_{I_n})$$

is used in equation 7 for normalization to eliminate the impact on the matching scores of the total peak intensities in MS/MS spectra.

The unknown MS/MS spectrum was assigned to the LM and/or potentially novel LM that has the highest matching score in addition to having the predicted UV spectral and chromatographic features (e.g., λ_{\max} and CRTs). This theoretical system was used successfully to identify 15-HETE in murine spleen (Fig. 3). Peak III displayed at CRT of 20.4 min on the chromatogram (at m/z 219 of MS/MS 319; left inset) and had a UV λ_{\max} of 235 nm (Fig. 3A, middle inset). Therefore, the search on the theoretical system was narrowed to the subdatabase with molecular ion m/z 319, UV λ_{\max} 235 nm, and CRT 21 min. In this case example, 15-HETE gave the highest matching score among all compounds in the subdatabase (Fig. 3B). The MS/MS peaks identified were annotated with the ion interpretation that also shows a fragmentation mechanism (Fig. 3A). Segments of 15-HETE that matched the MS/MS peaks according to the fragmentation rules are italicized (Fig. 3B). For comparison, MassFrontier was also used to identify peak III, which also identified it as 15-HETE (Fig. 3C).

Evaluation of LC-UV-MS/MS mediator-lipidomic databases and algorithms

We used LC-UV-MS/MS chromatograms and spectra acquired from murine tissue and organ extracts spiked with 34 LMs and related compounds for the evaluation. For every known compound added (i.e., spiked) in all samples, the search of its LC-UV-MS/MS data through a database gives a “hit list” showing what compound matches best. The best match has the highest matching score using the MassFrontier or theoretical database and the smallest contrast angle using COCAD. Hence, the best match is either correct or incorrect. The mean and SEM of percentage correct for best match indicated the performance of each database and algorithm (Table 1). Generally, COCAD offered the greatest percentage correct (Table 1), which was reasonable because COCAD takes into account both MS/MS ion intensities and identities measured from authentic eicosanoid standards and unknowns. The percentage correct from the theoretical system is comparable with that from the MassFrontier system (Table 1).

Only the identified ions were used for the COCAD and theoretical databases. The test results in Table 1 demonstrate that it is not necessary to use all of the MS/MS ions to identify a LM or other compounds. Moreover, in some cases it is not obvious and cost-efficient to identify all MS/MS ions. Rigorous identification can be done using isotope labeling and derivatization, which may not be feasible or realistic for routine analyses of the biologically relevant samples. We can identify a LM with precision using one or several chain-cut ions per functional group along with peripheral-cut ions and chain-plus-peripheral-cut ions according to the MS/MS fragmentation rules. For exam-

ple, we use at least four ions for monohydroxy-containing eicosanoids, six ions for dihydroxy-containing eicosanoids, and eight ions for trihydroxy-containing eicosanoids. Along these lines, John Beynon and coworkers originated the Eight Peak Index of Mass Spectra database for manual identification of compounds (as reviewed in 26). For different amounts of LMs added to the samples (1, 2.5, and 5 ng), the percentage identified correctly was not significantly different. Based on the test experiments using the theoretical database and algorithm, the average matching score for correct best match is 2.02 with a standard error of 0.71 ($n = 212$). Therefore, the threshold score for a 95% confidence interval of matching score for correct best match is $2.02 - 1.96 \times 0.71 = 0.62$.

The databases and search algorithms were developed on the basis of LC-UV-MS/MS data of LMs. The ion intensity patterns of MS/MS spectra generated from an ESI-triple quadrupole mass spectrometer are quite similar to those from an ESI-ion trap mass spectrometer, because the collision energy for both types of instruments is in the low-energy region [a few to 100 eV (laboratory kinetic energy of ions)] (7, 19, 20, 27). Therefore, the constants and algorithms described in this report may fit the CID spectra from triple quadrupole MS/MS without much modification. For high-collision-energy (10^2 to $\sim 10^3$ eV) CID spectra generated via sector or spectrum time-of-flight/time-of-flight analyzer, the relative intensity patterns are quite different compared with the low-energy spectra, although many ions occurred for both energy situations (7, 8, 19, 20, 27); for example, the peripheral-cut ions are less abundant than the chain-cut ions. For ion trap and triple quadrupole MS/MS, peripheral-cut ions are more abundant than chain-cut ions. Our constants and algorithms give chain-cut ions more weight than peripheral-cut ions because chain-cut ions are more important to define LM structures. Therefore, they may still fit high-collision-energy CID spectra. Nevertheless, the constants and algorithms should be thoroughly tested and modified accordingly to fit other instruments.

The CRTs used in this set of experiments were obtained using specified chromatographic conditions (for a column of 100 mm length and some for 150 mm length; see Systems and Methodology for details) and because several fundamental issues were our initial focus. Hence, the databases and algorithms were programmed so that the new LC-UV-MS/MS data, including other chromatographic conditions, can be easily entered and used in the databases.

CONCLUSIONS

Databases and search algorithms are imperative to identify LMs in a large number of complex biological samples by LC-UV-MS/MS. Integrating MS/MS spectra with UV spectra and chromatograms for LM identification as demonstrated in the present studies significantly improves the percentage identified correctly. For the three systems of databases and algorithms we constructed, only MS/MS spectra with UV spectra matched to the unknown were used

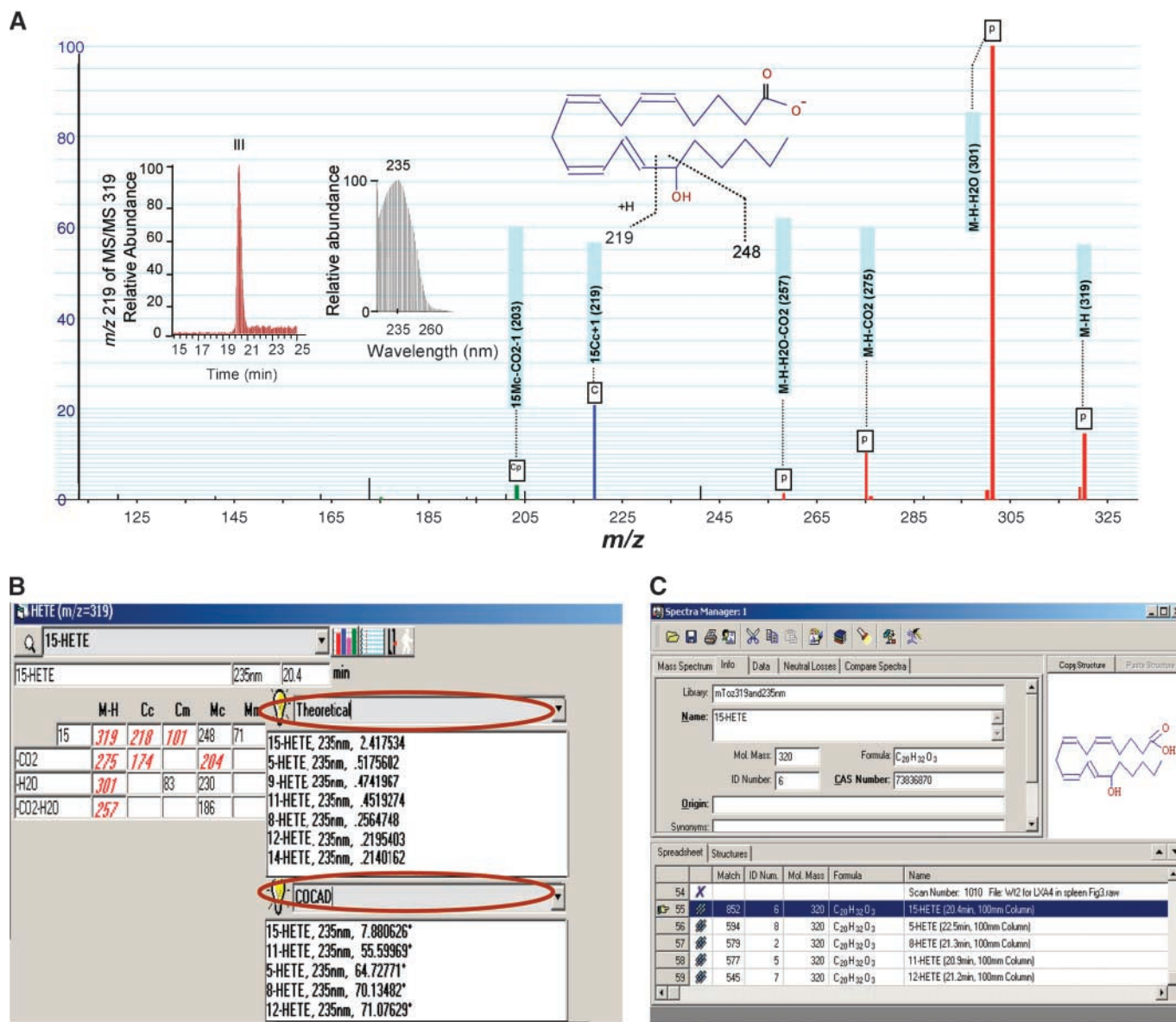



Fig. 3. Searching theoretical LC-UV-MS/MS databases indicated the presence of 15-hydroxy-eicosatetraenoic acid (15-HETE) in murine spleen. A: Identification and interpretation of anions in a MS/MS (at m/z 319) spectrum. The MS/MS scan conditions were as follows: parent ion, m/z 319; isolation width, 1.5; normalized collision energy, 42%; activation time, 30 ms; scan of MS/MS ions, from m/z 95 to 323 (see details in Systems and Methodology). C, chain-cut ion; Cp, chain-plus-peripheral-cut ion; P, peripheral-cut ion. Insets are for identified 15-HETE in the sample: left, chromatogram (at m/z 219 of MS/MS 319), which was the intensity temporal profile or extracted chromatogram for ion m/z 219 in the MS/MS spectrum of parent ion m/z 319 generated in ESI; middle, UV spectrum showing maximal absorption at 235 nm; right, proposed MS/MS segments on 15-HETE. The LC column was 100 mm long (see details in Systems and Methodology). B: Report for the search via the theoretical system shows that 15-HETE has the highest matching score; report for the search via COCAD shows that 15-HETE has the smallest contrast angle. C: 15-HETE also had the highest matching score when the LC-UV-MS/MS data were searched against the database built with MassFrontier.

for further searching. Next, the CRTs were matched for the compounds with a good match on both UV and MS/MS spectra. MS/MS ions were identified by the empirical fragmentation rules. The ion intensities were modified according to ion identities to calculate COCAD contrast angles and the theoretical matching score for database searching. The best performance was obtained with COCAD, which counts peak intensities differently based on ion identities during direct comparisons. Also, the theoretical systems presented here can be used to identify novel structures of

potentially new LMs without using standard LMs, with percentage correctly identified comparable with that of the system developed with MassFrontier when tested with LM chemical standards. Thus, the present results indicate that both the COCAD and theoretical systems can be used to provide identification and interpretations of negative-ion MS/MS fragmentation generated during profiling of LMs from complex biologic matrices.

The three mediator-lipidomic systems described in this report were constructed with results from LC-UV-MS/MS

obtained using specific LC conditions and parameters. Although these low-collision-energy CID spectra were quite similar to those acquired from triple quadrupole mass spectrometers (7, 19, 20), the lipidomic systems need to be thoroughly tested and modified wherever necessary to be useful with results from triple quadrupole mass spectrometers, not to mention those from intermediate- and high-collision-energy mass spectrometers. Theoretical databases and algorithms can be powerful when used appropriately to reduce significantly the tedious work that experienced biochemical researchers have to do when identifying the structures of novel LMs. However, they should consider other information or constraints, such as biosynthetic and metabolic pathways, stereochemistry, and bioactions, to ensure that the results are correct. Moreover, new LC results can be entered into the systems to extend the mediator-lipidomic systems for use with other LC conditions. Copies of the program and libraries can be made available to investigators on request. 

Many thanks to Mary Halm Small for expert editorial advice and assistance in manuscript preparation. The authors thank Katherine Gotlinger for laboratory assistance and Dr. Nan Chang for critiques. The authors also thank Dr. Lucila Ohno-Machado of BWH Bioinformatics and Decision Systems Group for helpful discussions. This work was supported in part by Grants GM-38765 (C.N.S.), P01 DE-13499 (C.N.S.), and P50 DE-016191 (S.H., Y.L., and C.N.S.) from the National Institutes of Health.

REFERENCES

- Serhan, C. N. 2002. Endogenous chemical mediators in anti-inflammation and pro-resolution. *Curr. Med. Chem.* **1**: 177–192.
- Serhan, C. N., C. B. Clish, J. Brannon, S. P. Colgan, N. Chiang, and K. Gronert. 2000. Novel functional sets of lipid-derived mediators with antiinflammatory actions generated from omega-3 fatty acids via cyclooxygenase 2-nonsteroidal antiinflammatory drugs and transcellular processing. *J. Exp. Med.* **192**: 1197–1204.
- Serhan, C. N., S. Hong, K. Gronert, S. P. Colgan, P. R. Devchand, G. Mirick, and R. L. Moussignac. 2002. Resolvins: a family of bioactive products of omega-3 fatty acid transformation circuits initiated by aspirin treatment that counter proinflammation signals. *J. Exp. Med.* **196**: 1025–1037.
- Hong, S., K. Gronert, P. R. Devchand, R. L. Moussignac, and C. N. Serhan. 2003. Novel docosatrienes and 17S-resolvins generated from docosahexaenoic acid in murine brain, human blood and glial cells: autocoids in anti-inflammation. *J. Biol. Chem.* **278**: 14677–14687.
- Balazy, M. 2004. Eicosanomics: targeted lipidomics of eicosanoids in biological systems. *Prostaglandins Other Lipid Mediat.* **73**: 173–180.
- Serhan, C. N. 2005. Mediator lipidomics. *Prostaglandins Other Lipid Mediat.* In press.
- Murphy, R. C., J. Fiedler, and J. Hevko. 2001. Analysis of nonvolatile lipids by mass spectrometry. *Chem. Rev.* **101**: 479–526.
- Griffiths, W. J., Y. Yang, J. Sjoevall, and J. Lindgren. 1996. Electrospray/collision-induced dissociation mass spectrometry of mono-, di- and tri-hydroxylated lipoxygenase products, including leukotrienes of the B-series and lipoxins. *Rapid Commun. Mass Spectrom.* **10**: 183–196.
- Wenk, M. R., L. Lucast, G. D. Paolo, A. J. Romanelli, S. F. Suchy, R. L. Nussbaum, G. W. Cline, G. I. Shulman, W. McMurray, and P. D. Camilli. 2003. Phosphoinositide profiling in complex lipid mixtures using electrospray ionization mass spectrometry. *Nat. Biotechnol.* **21**: 813–817.
- Lee, S. H., M. V. Williams, R. N. DuBois, and L. A. Blair. 2003. Targeted lipidomics using electron capture atmospheric pressure chemical ionization mass spectrometry. *Rapid Commun. Mass Spectrom.* **17**: 2168–2176.
- Chiang, N., T. Takano, C. B. Clish, N. A. Petasis, H. Tai, and C. N. Serhan. 2003. Aspirin-triggered 15-epi-lipoxin A₄ (ATL) generation by human leukocytes and murine peritonitis exudates: development of a specific 15-epi-LXA₄ ELISA. *J. Pharmacol. Exp. Ther.* **287**: 779–790.
- Lu, Y., S. Hong, E. Tjonahen, and C. N. Serhan. 2003. Lipid mediator lipidomics: database and search algorithm of electrospray ionization/tandem mass and ultraviolet spectra for structural elucidation. (5th Winter Eicosanoid Conference. Baltimore, MD, March 9–12, 2003).
- Stein, S. E., and D. R. Scott. 1994. Optimization and testing of mass spectral library search algorithms for compound identification. *J. Am. Soc. Mass Spectrom.* **5**: 859–866.
- Stein, S. E. 1995. Chemical substructure identification by mass spectral library searching. *J. Am. Soc. Mass Spectrom.* **6**: 644–655.
- Ausloos, P., C. L. Clifton, S. G. Lias, A. I. Mikaya, S. E. Stein, D. V. Tchekhovskoi, O. D. Sparkman, V. Zaikin, and D. Zhu. 1999. The critical evaluation of a comprehensive mass spectral library. *J. Am. Soc. Mass Spectrom.* **10**: 287–299.
- Mallard, G. W., and J. Reed. 1997. Automated mass spectral deconvolution and identification system. U. S. Department of Commerce, Technology Administration, National Institute of Standards and Technology, Gaithersburg, MD.
- Serhan, C. N. 1989. On the relationship between leukotriene and lipoxin production by human neutrophils: evidence for differential metabolism of 15-HETE and 5-HETE. *Biochim. Biophys. Acta.* **1004**: 158–168.
- Kiss, L., E. Bieniek, N. Weissmann, H. Schütte, U. Sibelius, A. Günther, J. Bier, K. Mayer, K. Henneking, W. Padberg, H. Grimm, W. Seeger, and F. Grimminger. 1998. Simultaneous analysis of 4- and 5-series lipoxygenase and cytochrome P450 products from different biological sources by reversed-phase high-performance liquid chromatographic technique. *Anal. Biochem.* **261**: 16–28.
- Serhan, C. N., A. Jain, S. Marleau, C. Clish, A. Kantarci, B. Behbehani, S. P. Colgan, G. L. Stahl, A. Merched, N. A. Petasis, L. Chan, and T. E. Van Dyke. 2003. Reduced inflammation and tissue damage in transgenic rabbits overexpressing 15-lipoxygenase and endogenous anti-inflammatory lipid mediators. *J. Immunol.* **171**: 6856–6865.
- Aliberti, J., S. Hieny, C. R. Sousa, C. N. Serhan, and A. Sher. 2002. Lipoxin-mediated inhibition of IL-12 production by DCs: a mechanism for regulation of microbial immunity. *Nat. Immunol.* **3**: 76–82.
- Levy, B. D., K. Gronert, C. B. Clish, and C. N. Serhan. 1999. Leukotriene and lipoxin biosynthesis. In *Lipid Second Messengers*. S. G. Laychock and R. P. Rubin, editors. CRC Press, Boca Raton, FL. 83–111.
- MassFrontier™ version 2.0 user manual. 1998–2000. HighChem, Ltd., Finnigan Mat, San Jose, CA.
- McLafferty, F. W., and F. Turecek. 1993. Elemental composition. In *Interpretation of Mass Spectra*. 4th edition. I. Imfeld and A. Kelly, editors. University Science Books, Mill Valley, CA. 19–34.
- Wan, K. X., I. Vidavsky, and M. L. Gross. 2002. Comparing similar spectra: from similarity index to spectral contrast angle. *J. Am. Soc. Mass Spectrom.* **13**: 85–88.
- LCQ™ user manual. 1996. Finnigan Mat, San Jose, CA.
- McLafferty, F. W., D. A. Stauffer, S. Y. Loh, and C. Wesdemiotis. 1999. Unknown identification using reference mass spectra: quality evaluation of databases. *J. Am. Soc. Mass Spectrom.* **10**: 1229–1240.
- Wheeler, P., J. A. Zirrollo, and R. C. Murphy. 1996. Electrospray ionization and low energy tandem mass spectrometry of polyhydroxy unsaturated fatty acids. *J. Am. Soc. Mass Spectrom.* **7**: 140–149.